the $Mn^{II}Mn^{III}Mn^{IV}Mn^{II}$ oxidation-state assignment. Supporting this assignment is the electronic spectrum of **1** in CH_3CN, which, in the visible region, closely resembles other species that contain the $\{Mn_2O_2\}^{3+}$ core.[15] As was the case for $\{[Mn_2(TPHPN)(O_2CCH_3)(H_2O)]_2O\}^{4+}$,[6] the N_3 ends of the TPHPN ligands bind in a meridional manner. The Mn^{III}–O_{oxo} bond distances in the inner $Mn_2(\mu\text{-}O)_2$ core of **1** are comparable to corresponding parameters in several crystallographically characterized di-μ-oxo dimers.[11] Shortening of the Mn–O_{oxo} bonds is accompanied by elongation along the N(1)–Mn(1)–N(3) axis.[12] The Mn(2)–O(3) bond length (2.109 (3) Å) is 0.065 Å shorter than the Mn^{III}–H_2O distances in $[Mn_2O(O_2CCH_3)_2(H_2O)_2(bpy)_2]^{2+}$.[13] Furthermore, the coordinated water molecules in **1** are involved in an intermolecular hydrogen bonding interaction to the bridging oxo moieties (O(2)), with contacts of 2.596 (5) Å.[14] Both H atoms of the H_2O ligand were located on a difference Fourier map. It is interesting to note that the O(2)···O(2′) contact (2.454 (5) Å) is actually somewhat shorter than the O(2)···O(3) separation.

Cyclic voltammetry of **1** in CH_3CN solution, using $(Et_4N)(ClO_4)$ as supporting electrolyte, reveals two quasi-reversible redox waves with $E_{1/2}$ values of 0.36 V ($E_{p,a} - E_{p,c}$ = 0.24 V) and 0.87 V ($E_{p,a} - E_{p,c}$ = 0.27 V) vs SSCE. On the basis of spectroelectrochemical studies,[15] the wave at 0.87 V is assigned to an oxidation of **1** and the wave at 0.36 V is assigned to a reduction to the $Mn^{III}_2Mn^{II}_2$ oxidation level. Magnetic susceptibility measurements on a solid sample of **1** indicate a moment of 8.7 μ_B per molecule at 279 K, decreasing to 6.6 μ_B at 7 K. Since the spin-only moment for four magnetically uncoupled manganese ions is 10.4 μ_B ($2 \times Mn^{II} + Mn^{III} + Mn^{IV}$), the above values are consistent with net antiferromagnetic interactions within the tetranuclear aggregate.

The relatively short intramolecular O(2)···O(3) interaction in **1** gives rise to the notion that bond formation between these atoms may be promoted by an oxidation/deprotonation process as shown in Scheme I. We suggest that this mechanism represents a plausible pathway by which the key O–O bond-forming step in PSII OEC water oxidation may occur. Compound **1** corresponds to a model for the S_0 oxidation level in the Kok S-state scheme.[16] While heretofore oxidation-state assignments for a given S state generally avoid formulations with both Mn^{II} and Mn^{IV} present, the stability of **1** demonstrates that, with appropriate donors, manganese atoms at these oxidation levels can coexist in the same molecule. Further characterization of **1** and its oxidized and deprotonated derivatives is underway.

Acknowledgment. This work was supported by Grant No. GM382751-01 from the National Institutes of General Medical Sciences. W.H.A. is grateful for a Searle Scholars Award (1986–1989).

Note Added in Proof. It has come to our attention that Professor M. Suzuki and co-workers have isolated the title complex as a perchlorate salt. We are grateful to them for supplying us with a preprint of their manuscript (submitted to *Chem. Lett.*) which describes this work.

Registry No. 1 $(CF_3SO_3)_3 \cdot 3CHCl_3$, 127103-44-0; **1** $(CF_3SO_3)_3$, 127103-43-9; $[Mn_4O_2(TPHPN)_2(H_2O)_2(ClO_4)_2](ClO_4)_3$, 127129-91-3; H_2O, 7732-18-5.

(12) The fact that the elongation is not as pronounced as often observed is presumably due to averaging of the Mn^{III} and Mn^{IV} sites by static disorder in the crystal lattice.

(13) Ménage, S.; Girerd, J.-J.; Gleizes, A. *J. Chem. Soc., Chem. Commun.* **1988**, 431–432.

(14) Hydrogen bonding of the coordinated water molecules to the oxo bridge in **1** is reminiscent of the hydrogen bonding of hydroperoxide to the bridging oxo group in oxyhemerythrin.[3c]

(15) Compound **1** as isolated has an electronic spectrum similar to the spectra of other species that have $\{Mn_2O_2\}^{3+}$ cores (in CH_3CN, λ, nm (ϵ, M^{-1} cm^{-1}): 547 (760), 625 (520)).[11c] When a platinum electrode is poised at −0.1 V vs SSCE in a CH_3CN solution of **1**, current passes and the visible absorption diminishes markedly. On the other hand, when the electrode is held at +1.3 V vs SSCE, the absorption in the visible region increases strongly as current is passed. Both of these processes are reversible on the time scale of approximately 1 h.

(16) Full details of the proposed mechanism will be presented elsewhere.

Supplementary Material Available: A fully labeled ORTEP drawing, atomic positional and thermal parameters, and intramolecular distances and angles for $[Mn_4O_2(TPHPN)_2(H_2O)_2(CF_3SO_3)_2](CF_3SO_3)_3 \cdot 3CHCl_3$ (14 pages). Ordering information is given on any current masthead page.

Synthetic and Mechanistic Studies on Esperamicin A_1 and Calicheamicin γ_1. Molecular Strain Rather Than π-Bond Proximity Determines the Cycloaromatization Rates of Bicyclo[7.3.1] Enediynes

Philip Magnus,*,† Simon Fortt, Thomas Pitterna, and James P. Snyder*,‡

Department of Chemistry, University of Texas at Austin Austin, Texas 78712
Drug Design, Searle Research and Development 4901 Searle Parkway, Skokie, Illinois 60077

Received February 19, 1990

During the past two years there has been intense interest in the remarkable antitumor antibiotics esperamicin A_1 (**1**) and calicheamicin γ_1 (**2**).[1] These unusual natural products exert their DNA cleaving properties by binding into the minor groove. In some as yet unspecified manner the allylic trisulfide is subsequently cleaved in situ to release the thiol (or thiolate) **3**. The latter undergoes conjugate addition to the proximate α,β-unsaturated carbonyl system (C-1) to give **4**. With sp^3 hybridization at C-1 the bicyclic enediyne no longer violates Bredt's rule; the transition state leading to 1,4-diyl **5** becomes energetically feasible. Hydrogen atom abstraction from the ribose backbone by the biradical results in single- and double-stranded-DNA cleavage and formation of the cycloaromatized adduct **6** (Scheme I).

It has been suggested that rehybridization at C-1 ($sp^2 \rightarrow sp^3$) results in contraction of the C-6/C-11 distance ($r(C_{sp}\cdots C_{sp})$) from 3.35 Å to 3.16 Å, causing spontaneous, ambient cycloaromatization to 1,4-diyl **5**. These conclusions were based on a study of monocyclic enediynes.[2] Alternatively, qualitative investigations led us to propose that an overall change in strain energy from enediyne to cycloaromatized adduct furnishes the closure driving force.[3] More recently, we presented computational evidence that factors controlling the ease of cycloaromatization are directly related to strain energy in the transition state rather than to proximity of the acetylenic carbon atoms (r) in the ground state.[4] Quantitative experimental and theoretical data reported herein support the strain attenuation hypothesis.

† University of Texas at Austin.
‡ Searle Research and Development.

(1) The structures of the esperamicins and calicheamicins were reported in 1987. Golik, J.; Dubay, G.; Groenewold, G.; Kawaguchi, H.; Konishi, M.; Krishnan, B.; Ohkuma, H.; Saitoh, K.; Doyle, T. W. *J. Am. Chem. Soc.* **1987**, *109*, 3462. Lee, M. D.; Dunne, T. S.; Siegel, M. M.; Chang, C. C.; Morton, G. O.; Borders, D. B. *J. Am. Chem. Soc.* **1987**, *109*, 3464. Lee, M. M.; Dunne, T. S.; Chang, C. C.; Ellestad, G. A.; Siegel, M. M.; Morton, G. O.; McGahren, W. G.; Borders, D. B. *J. Am. Chem. Soc.* **1987**, *109*, 3466. For other synthetic approaches, see: Danishefsky, S. J.; Mantlo, N. B.; Yamashita, D. S.; Schultz, G. *J. Am. Chem. Soc.* **1988**, *110*, 6980. Schreiber, S. L.; Kiessling, L. L. *Tetrahedron Lett.* **1989**, *30*, 433. Kende, A. S.; Smith, C. A. *Tetrahedron Lett.* **1988**, *29*, 4217. Nicolaou, K. C.; Ogawa, Y.; Zuccarello, G.; Kataoka, H. *J. Am. Chem. Soc.* **1988**, *110*, 7247. Tomioka, K.; Fujita, H.; Koga, K. *Tetrahedron Lett.* **1989**, *30*, 851. Schoenen, F. G.; Porco, J. A., Jr.; Schreiber, S. L.; VanDuyne, G. D.; Clardy, J. *Tetrahedron Lett.* **1989**, *30*, 3765. Haseltine, J. N.; Danishefsky, S. J.; Schulte, G. *J. Am. Chem. Soc.* **1989**, *111*, 7638. Synthesis of calicheamicinone: Cabal, M. P.; Coleman, R. S.; Danishefsky, S. J. *J. Am. Chem. Soc.* **1990**, *112*, 3253.

(2) Nicolaou, K. C.; Zuccarello, G.; Ogawa, W.; Schweiger, E. J.; Kumazawa, T. *J. Am. Chem. Soc.* **1988**, *110*, 4866.

(3) Magnus, P.; Carter, P. A. *J. Am. Chem. Soc.* **1988**, *110*, 1626. Magnus, P.; Lewis, R.; Huffman, J. C. *J. Am. Chem. Soc.* **1988**, *110*, 6921.

(4) Snyder, J. P. *J. Am. Chem. Soc.* **1989**, *111*, 7630.

0002-7863/90/1512-4986$02.50/0

Scheme I

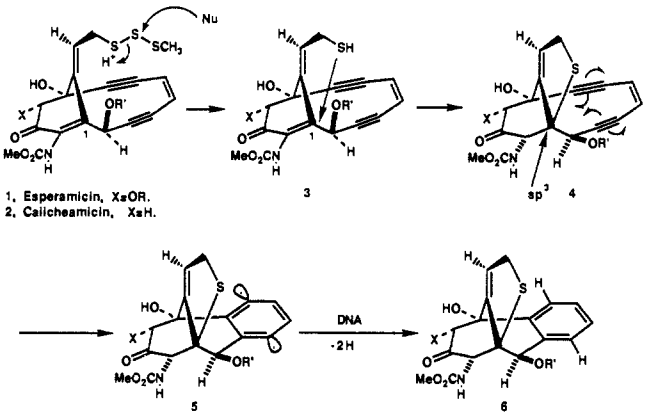

Scheme II[a]

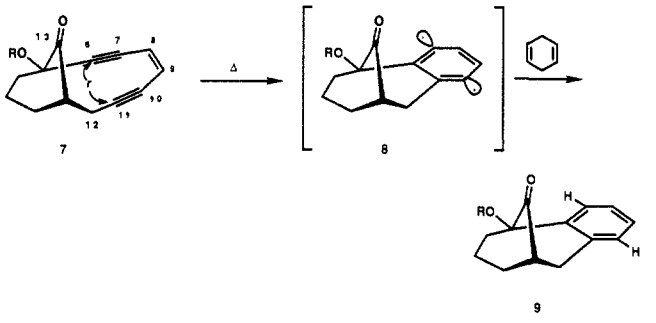

[a] R = *t*-BuMe$_2$Si.

Table I. Kinetic Parameters for the Thermal Cyclization of Enediyne **7**

T, °C	*k*, s^{-1}	$t_{1/2}(\tau)$
71	1.07×10^{-4}	2.10 h
79	2.56×10^{-4}	45 min
87	5.00×10^{-4}	23 min
95	1.16×10^{-3}	10 min
104	2.58×10^{-3}	4.30 min

The crystalline 13-keto bicyclo[7.3.1] enediyne **7** has been characterized by X-ray crystallography, r = 3.391 Å. The six-membered ring is captured in a boat conformation in the crystal (Scheme II). Heating a solution of **7** in 1,4-cyclohexadiene at temperatures ranging from 71 °C to 104 °C and monitoring both the rate of disappearance of **7** and the rate of formation of **9** (>70%) gave the *first-order* rate constants shown in Table I. Extrapolated to 37 °C, the thermodynamic parameters are $\Delta G^{\ddagger}$ = 26.3 kcal mol^{-1}, $\Delta H^{\ddagger}$ = 24.0 kcal mol^{-1}, $\Delta S^{\ddagger}$ = −7.33 eu, E_a = 24.6 kcal mol^{-1}, and $k = 1.85 \times 10^{-6}$ s^{-1} (error ±2%).

The five-membered-ring analogue of **7**, namely, 12-keto bicyclo[7.2.1] enediyne **10**, was readily made in the same way as **7** except that the starting material was cyclopentane-1,2-dione. The (*E*)-oxime **11** gave suitable crystals for X-ray analysis. The C-5/C-10 separation is r = 3.368 Å (vs 3.391 Å for **7**). Although the distance between the two acetylenic carbons is almost within the range postulated for ambient cycloaromatization (<3.35 Å) and below r in **7**, compound **10** is remarkably resistant to ring closure. At 124 °C (averaged over five runs), $k = 2.08 \times 10^{-5}$ s^{-1} for conversion of **10** into the bicyclo[3.2.1] system **12** (73%). This corresponds to a $\Delta G^{\ddagger}$(124 °C) of 32.0 kcal mol^{-1} and gives $\Delta\Delta G^{\ddagger}$(**10**–**7**) = 5.1 ± 0.2 kcal mol^{-1} at the same temperature. In other words, even though r is less in **10** than in **7**, it *cycloaromatizes 650 times more slowly* at 124 °C. By contrast, the cycloaromatization rate of alcohol **13** to **14** at 85 °C (k = 1.467 × 10^{-4} s^{-1}) is *216 times faster* than the rate for **10** and *one-third* the rate for **7** ($\Delta G^{\ddagger}$ = 27.4 kcal/mol). The alcohol derived from **7** cycloaromatizes rapidly at 0 °C.

The kinetic observations can be readily interpreted within the recently described transition-state model for enediyne cyclization.[4] As a preliminary step, torsional isomerism (C(O)C–OR) for structures **7**, **10**, and **13** (R = CH$_3$) and the corresponding biradicaloid transition states was examined by MM2/PRDDO to locate the global minima. Within this framework the PRDDO energy barriers are calculated as ΔE^{*} = *TS*(GVB) − *GS*(SCF). Low-energy conformations for the three structures yield ΔE^{*} = 25.4, 31.2, and 27.5 kcal, respectively. In close agreement with experiment, $\Delta\Delta E^{*}$(**10**–**7**) = 5.8 kcal.[5] The large barrier differential is a result of two separate strain components. The first is estimated by excising the cyclopentanone and cyclohexanone units from **10** and **7** and the corresponding transition states for comparison with the strain-free rings obtained by MM2 optimization. In all cases the cycloalkanones constrained to their dihedral angles in the substituted bicycles are destabilized by 1–9 kcal (PRDDO). Secondly and more importantly, while the five-ring energy increases by 1.5 kcal as it moves from enediyne **10** to a biradicaloid transition state, the six-membered ring of **7** drops by 6.0 kcal (boat → chair) along the same route. At the biradicaloid transition state for closure of **7**, the whole-molecule $\Delta\Delta E^{*}$(boat–chair) = 3.5 kcal. Thus the cyclohexanone derivative **7** enjoys a conformationally activated strain-release mechanism from ground to transition state unavailable to the cyclopentanone skeleton.

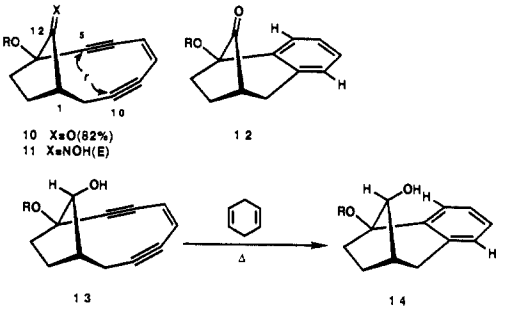

Similar considerations apply to the cyclization of bicyclic alcohol **13** and the corresponding alcohol from **7**. Intermediate strain reduction in the transition state for **13** (−1.5 kcal for the five-membered ring) accounts for its kinetic stability relative to **7** and **10** (R = CH$_3$); $\Delta\Delta E^{*}$(**13**–**10**) = −3.7 and $\Delta\Delta E^{*}$(**13**–**7**) = 2.1 kcal. The six-membered-ring alcohol from **7** is computed to show ΔE^{*} = 22.0 kcal, in agreement with its rapid disappearance at 0 °C. In this case the cyclohexanol ring boat → chair inversion is estimated to elicit a strain relief of 6.1 kcal at the activated complex.

In summary, the cyclization rates of bicyclic enediynes are best interpreted as governed by strain-energy modulation in the pseudocyclic transition state. In a broader context, of course, it is the difference in strain between enediyne and the biradicaloid that determines the closure tendency. As described in the accompanying paper, monocyclic enediynes are subject to the same principles.

The above considerations will be of paramount importance for the design of enediyne analogues that can aromatize under physiological conditions.[6]

Acknowledgment. The National Institutes of Health and the Welch Foundation are thanked for their support. Dr. Vince Lynch is thanked for the X-ray structure determination of **11**.

Supplementary Material Available: Spectral data for compounds **10**–**14** and details of the X-ray structural determination of **11** (18 pages). Ordering information is given on any current masthead page.

(5) This considerable activation energy difference was foreshadowed by the model prior to synthesis[4] and explicitly predicted prior to kinetic measurement.

(6) **Note Added in Proof**: Townsend has recently measured the rate of cycloaromatization of the dihydrothiophene **4** into **6** and finds the first-order rate constant equal to 3.7 ± 0.5 × 10^{-4} s^{-1}; $\Delta G^{\ddagger}$ = 19.4 kcal/mol. DeVoss, J. J.; Hangeland, J. J.; Townsend, C. A. *J. Am. Chem. Soc.* In press.